Attractively bound pairs of atoms in the Bose-Hubbard model and antiferromagnetism

Bernd Schmidt, Michael Bortz, Sebastian Eggert, and Michael Fleischhauer
Fachbereich Physik, Technische Universität Kaiserslautern, D-67663 Kaiserslautern, Germany

David Petrosyan
Institute of Electronic Structure & Laser, FORTH, 71110 Heraklion, Crete, Greece

(Dated: February 25, 2009)

We consider a periodic lattice loaded with pairs of bosonic atoms tightly bound to each other via strong attractive on-site interaction that exceeds the inter-site tunneling rate. An ensemble of such lattice-dimers is accurately described by an effective Hamiltonian of hard core bosons with strong nearest-neighbor repulsion which is equivalent to the XXZ model with Ising-like anisotropy. We calculate the ground-state phase diagram for a one-dimensional system which exhibits incompressible phases, corresponding to an empty and a fully filled lattice (ferromagnetic phases) and a half-filled alternating density crystal (anti-ferromagnetic phase), separated from each other by compressible phases. In a finite lattice the compressible phases show characteristic oscillatory modulations on top of the anti-ferromagnetic density profile and in density-density correlations. We derive a kink model which provides simple quantitative explanation of these features. To describe the long-range correlations of the system we employ the Luttinger liquid theory with the relevant Luttinger parameter K obtained exactly using the Bethe Ansatz solution. We calculate the density-density as well as first-order correlations and find excellent agreement with numerical results obtained with density matrix renormalization group (DMRG) methods. We also present a perturbative treatment of the system in higher dimensions.

PACS numbers: 37.10.Jk, 03.75.Lm, 05.30.Jp, 75.10.Jm

I. INTRODUCTION

Various idealized models describing many-body quantum systems on a lattice, such as the Heisenberg spin and Hubbard models, have been widely studied for decades in condensed matter physics [1, 2]. With the recent progress in cooling and trapping bosonic and fermionic atoms in optical lattices [3], some of these models can now be realized in laboratory with unprecedented accuracy—the Hubbard model being a case in point [4]. Implementing more general models, e.g., extended Hubbard or asymmetric spin models, with atoms in optical lattice potentials is, however, more challenging but potentially very rewarding. The purpose of the present paper is to study an experimentally relevant situation realizing the extended Hubbard model or, equivalently, an anti-ferromagnetic XXZ model in the Ising-like phase with cold neutral atoms in a deep optical lattice potential.

We consider an optical lattice realization of the Bose-Hubbard model with strong on-site attractive interaction between the atoms. Specifically, we study a situation when each site of the lattice is loaded with either zero or two atoms. Experimentally, this can be accomplished by adiabatically dissociating a pure sample of Feshbach molecules in a lattice with at most one molecule per site [5, 6]. The on-site attractive interaction then results in the formation of attractively-bound atom pairs [7, 8]—"dimers",— whose repulsive analog was realized in a recent experiment [6].

For strong atom-atom interaction, either attraction or repulsion, the dimer constituents are well co-localized [8], and an ensemble of such dimers in a lattice can be accurately described by an effective Hamiltonian which has the form of a spin-$\frac{1}{2}$ XXZ model with Ising-like anisotropy. The derivation of the effective Hamiltonian is given in [9], where we have also discussed its properties for the case of repulsive atom-atom interactions. Since the resulting nearest-neighbor attraction of dimers dominates the kinetic energy, it causes the formation of minimal surface "droplets" of dimers on a lattice below a critical temperature. In the case of attractive atom-atom interaction considered here, the interaction between the nearest neighbor dimers is a strong repulsion. We then find that the ground state of the system of dimers in a grand canonical ensemble exhibits incompressible phases, corresponding to an empty and a fully filled lattice as well as a half-filled alternating density crystal. These phases are separated from each other by compressible phases.

We calculate numerically and analytically the ground state phase diagram for this system in one dimension (1D). The critical points can be obtained with the help of the Bethe Ansatz making use of the correspondence to the XXZ model [10]. In a finite lattice and close to half filling, the compressible phases show characteristic oscillatory modulations on top of the anti-ferromagnetic density profile. A simple kink model is derived which explains the density profiles as well as number-number correlations in the compressible phases. The long-range correlations of the dimer system show a Luttinger liquid behavior. We calculate the amplitude and density correlations in a finite system from a field theoretical model, which show excellent agreement with the numerical data. The corresponding Luttinger parameter is obtained by solving the Bethe integral equations. We then proceed to a perturbative treatment of the system in higher di-

mensions. Finally, we briefly discuss the implications of tunable nearest-neighbour interactions.

II. EFFECTIVE DIMER MODEL

We consider attractively-bound dimers on a d-dimensional isotropic lattice. Because of the strong on-site atom-atom interaction $U < 0$, it is energetically impossible to break the dimers, which effectively play the role of hard core bosons on the lattice. Via a second order process in the original atom hopping J, the dimers can tunnel to neighboring sites with the rate $\tilde{J} \equiv -2J^2/U > 0$ and carry nearest neighbor interaction fixed at $4\tilde{J}$. The effective Hamiltonian for the system has been derived in [9],

$$\hat{H}_{\rm eff} = \sum_j \left(2\epsilon_j + U - 2d\tilde{J}\right)\hat{m}_j - \tilde{J}\sum_{\langle j,i\rangle} \hat{c}_j^\dagger \hat{c}_i + 4\tilde{J}\sum_{\langle j,i\rangle} \hat{m}_j\hat{m}_i, \tag{1}$$

where $\hat{c}_j^\dagger$ and $\hat{c}_j$ are the creation and annihilation operators and $\hat{m}_j = \hat{c}_j\hat{c}_i$ is the number operator for a dimer at site j. In the first term of Eq. (1), the local potential energy $2\epsilon_j$ of the pair of atoms is modified by an additional "internal energy" of the dimer $\left(U - 2d\tilde{J}\right)$, which is negative for attractive interactions, so that the effective local chemical potential is given by $\mu_j = |U| + 2d\tilde{J} - 2\epsilon_j$. The kinetic energy of one dimer described by the second term of Eq. (1) spans the interval $[-2d\tilde{J}, 2d\tilde{J}]$ corresponding to a Bloch band of a d dimensional square lattice. In comparison, bringing a pair of dimers to neighboring sites requires an energy of $8\tilde{J}$ due to the strong repulsive interaction in the last term.

Since the dimers are effectively hard-core bosons, it is possible to map the above Hamiltonian onto a spin system. Mapping between bosons and spin operators is given by the well known Holstein Primakoff transformation

$$\begin{aligned} \hat{S}_j^z &= \hat{m}_j - 1/2, \\ \hat{S}_j^+ &= \hat{c}_j^\dagger \sqrt{1-\hat{m}_j}, \\ \hat{S}_j^- &= \sqrt{1-\hat{m}_j}\,\hat{c}_j, \end{aligned} \tag{2}$$

which preserves the SU(2) commutation relations exactly. Since double occupancy is forbidden, $m_j = 0$ or 1, the factor $\sqrt{1-\hat{m}_j}$ is zero for an occupied site and unity for an empty site. Therefore, we simply have $\hat{S}_j^+ = \hat{c}_j^\dagger$ and $\hat{S}_j^- = \hat{c}_j$, so that the equivalent Hamiltonian is given by

$$\hat{H}_{\rm spin}/\tilde{J} = -\sum_{\langle j,i\rangle}\left(\hat{S}_i^+\hat{S}_j^- - 4\hat{S}_i^z\hat{S}_j^z\right) + \sum_j h_j\hat{S}_j^z, \tag{3}$$

with an effective field of $h_j = (2\epsilon_j + U)/\tilde{J} + 6d$. This is the anti-ferromagnetic XXZ spin model with a fixed anisotropy of 4, i.e., the model is in the gapped Ising-like phase. A given total number N of dimers in a lattice of N_s sites corresponds, in the spin model, to a fixed total magnetization $M_z = N - \frac{1}{2}N_s$.

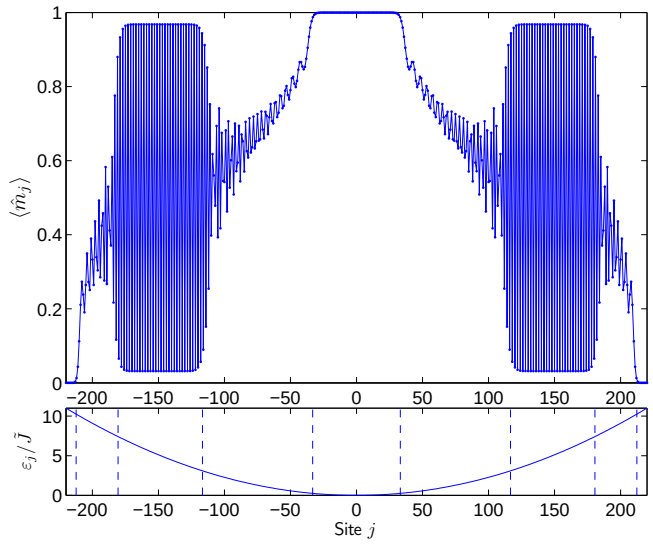

FIG. 1: (Color online) Density of dimers in a 1D lattice and additional harmonic confinement potential obtained from DMRG simulation, with $\mu_j = 18.5\tilde{J} - 2\epsilon_j$ and $\epsilon_j/\tilde{J} = j^2/4400$. One clearly identifies the incompressible phase with homogeneous filling of $\langle\hat{m}_j\rangle = 1$ in the trap center, and two AF phases, separated by compressible intermediate regions.

III. DIMER SYSTEM IN ONE DIMENSION

It is now clear that the behaviour of the dimer system in one dimension can be determined via isomorphic mapping of Eq. (1) onto the 1D integrable XXZ model in a uniform field,

$$\hat{H}_{XXZ} = -\sum_{j=1}^{N_s-1}\left(\hat{S}_j^x\hat{S}_{j+1}^x + \hat{S}_j^y\hat{S}_{j+1}^y - \Delta\hat{S}_j^z\hat{S}_{j+1}^z\right) + h\sum_{j=1}^{N_s}\hat{S}_j^z, \tag{4}$$

where Δ is the anisotropy of the spin-spin interaction.

A. Ground-state phase diagram

An important general feature of the dimer model in Eq. (1) is that the ratio of interaction to kinetic energy has a fixed value larger than one. As a consequence, the ground-state of the system is interaction dominated giving rise to interesting correlation properties.

In a homogeneous system, the ground-state of the system depends only the overall chemical potential $\mu/\tilde{J}$. The corresponding phase diagram can be completely mapped out in an experiment by adding a shallow external trapping potential with sufficiently small confinement such that the local density approximation is valid and $\mu = |U| + 2\tilde{J} - 2\epsilon_j$ does not change significantly over many lattice sites. Then different regions in the trap would correspond to different chemical potentials.

In Fig. 1 we plot the density of dimers in a one-dimensional lattice and an additional harmonic trapping

potential obtained by numerical DMRG calculations [11]. One clearly recognizes three types of regions: In the trap center, where the local chemical potential is largest, there is a unit filling of dimers. Separated by a spatial region of monotonously decreasing average filling follows a region where the filling is exactly one half and the dimers form a periodic pattern with period 2 and almost maximum modulation depth. In this region, the dominant effect is the nearest neighbour repulsion $4\tilde{J} > 0$ of Eq. (1). Towards the edge of the dimer cloud, the average density decreases again monotonously to zero. In terms of the equivalent spin system, the central region corresponds to a gapped phase of full spin polarization caused by a large negative effective magnetic field. The region of exactly one half average filling corresponds to another gapped phase with anti-ferromagnetic (AF) order induced by the strong, Ising-like interaction $-4\hat{S}^z_j\hat{S}^z_{j+1}$ of Eq. (3). The intermediate regions are compressible.

The critical values of the chemical potential for the transitions between compressible and incompressible phases in 1D are known from the work of Yang and Yang [10] on the XXZ model of Eq. (4). For the parameters of the present system, we have

$$\mu_\downarrow/\tilde{J} = -2, \tag{5a}$$

$$\mu_{\mathrm{AF}-}/\tilde{J} = 8 - 2\sqrt{15}\sum_{n=-\infty}^{\infty}\frac{(-1)^n}{\cosh\left(n\,\mathrm{arccosh}(4)\right)} \approx 3.68361\ldots, \tag{5b}$$

$$\mu_{\mathrm{AF}+}/\tilde{J} = 8 + 2\sqrt{15}\sum_{n=-\infty}^{\infty}\frac{(-1)^n}{\cosh\left(n\,\mathrm{arccosh}(4)\right)} \approx 12.31638\ldots, \tag{5c}$$

$$\mu_\uparrow/\tilde{J} = 18. \tag{5d}$$

These values agree very well with those obtained from exact diagonalization on a small homogeneous lattice with $N_s = 10$ sites and periodic boundary conditions, as well as DMRG simulation with up to $N_s = 300$ and open boundary conditions. They also match the different regions of Fig. 1.

B. Mott-insulating phases

In the language of spin Hamiltonian, phases with zero ($N = 0$) or full ($N = N_s$) filling correspond to ferromagnetic phases with a simple form of the ground state

$$|\psi_\downarrow\rangle = |\downarrow,\downarrow,\downarrow,\ldots,\downarrow\rangle, \tag{6}$$

$$|\psi_\uparrow\rangle = |\uparrow,\uparrow,\uparrow,\ldots,\uparrow\rangle. \tag{7}$$

Particle-hole excitations are not possible in the Mott-insulating state (7), while inserting a particle into (6) or removing one from (7), corresponding to flipping a spin, carries finite energy cost given by Eqs. (5a) and (5d). Hence these phases are incompressible.

For half filling ($N = \frac{1}{2}N_s$) the situation corresponds most closely to an AF phase. However, in this case the simple Néel state

$$|\psi^{(0)}_{\mathrm{AF}}\rangle = |\ldots,\downarrow,\uparrow,\downarrow,\uparrow,\downarrow,\uparrow,\downarrow,\uparrow,\ldots\rangle, \tag{8}$$

is not an exact eigenstate of the full Hamiltonian $\hat{H}_{\mathrm{eff}}$ in (1). Rather, $|\psi^{(0)}_{\mathrm{AF}}\rangle$ is an eigenstate of Hamiltonian $\hat{H}^{(0)}_{\mathrm{eff}} \equiv \hat{H}_{\mathrm{eff}} - \hat{H}_{\mathrm{hop}}$ without the hopping term $\hat{H}_{\mathrm{hop}} = -\tilde{J}\sum_j(\hat{c}^\dagger_{j+1}\hat{c}_j + \hat{c}^\dagger_j\hat{c}_{j+1})$. Due to $\hat{H}_{\mathrm{hop}}$ a dimer can tunnel from an occupied site to a neighboring empty site, which in terms of the Néel state (8), corresponds to flipping two neighboring spins, resulting in a state of the form

$$|\psi^{(1)}_j\rangle = |\ldots,\downarrow,\uparrow,\downarrow,\downarrow_j,\uparrow_{j+1},\uparrow,\downarrow,\uparrow,\ldots\rangle. \tag{9}$$

If we assume periodic boundary conditions and an even number of lattice sites N_s, there are $j = 1,\ldots,N_s$ different states (9), one for each link where two neighboring spins can be flipped. Each of those states $|\psi^{(1)}_j\rangle$ has a larger repulsive (Ising) interaction energy $E^{(1)}_j$, which is increased by $8\tilde{J}$ relative to energy $E^{(0)}_{\mathrm{AF}}$ of state $|\psi^{(0)}_{\mathrm{AF}}\rangle$. It is tempting to treat the the smaller hopping $\hat{H}_{\mathrm{hop}}$ as perturbation with respect to $\hat{H}^{(0)}_{\mathrm{eff}}$, but unfortunately already the first order correction carries a contribution from all N_s possible states in Eq. (9). In higher order perturbation theory the number of contributing states increases with higher powers in N_s, so that the perturbation series diverges in the thermodynamic limit.

However, if we are interested in local observables, such as the density in Fig. 1, it is possible to restrict the perturbation only to those hopping terms which change the value of the density at a particular point. In particular, in order to calculate the ground state expectation value of $\langle\psi_{\mathrm{AF}}|S^z_j|\psi_{\mathrm{AF}}\rangle$, we have to make the following ansatz for the ground state $|\psi_{\mathrm{AF}}\rangle$

$$|\psi_{\mathrm{AF}}\rangle \approx |\psi^{(0)}_{\mathrm{AF}}\rangle + \sum_{i=j-1}^{j}\frac{|\psi^{(1)}_i\rangle\langle\psi^{(1)}_i|\,\hat{H}_{\mathrm{hop}}\,|\psi^{(0)}_{\mathrm{AF}}\rangle}{E^{(0)}_{\mathrm{AF}} - E^{(1)}_i} = |\psi^{(0)}_{\mathrm{AF}}\rangle + \frac{1}{8}\left(|\psi^{(1)}_{j-1}\rangle + |\psi^{(1)}_j\rangle\right), \tag{10}$$

which can be normalized by a factor of $1/\sqrt{1+1/32}$. This state is in general a bad approximation to the ground state, but it describes very well which terms in the Hamiltonian affect the local density at site j, since higher order hopping only contributes 1/64 or less. Accordingly, the local density is given by

$$\langle\psi_{\mathrm{AF}}|S^z_j|\psi_{\mathrm{AF}}\rangle \approx (-1)^j\frac{32}{66}\left(1 - \frac{1}{32}\right) = (-1)^j\frac{31}{66} \tag{11}$$

which corresponds to a deviation of about 0.03 from perfect alternating order. Our numerical results for homogeneous systems show a deviation of about 0.032 which is in very good agreement with the prediction. Even though

the half filling state always implicitly contains excitations of type (9), the removal or addition of a particle still costs relatively large energy given by Eq. (5b) or (5c), which makes the AF phase incompressible.

C. Properties of compressible phases

In the remainder of this Section, we examine the compressible phases, mainly in the vicinity of the antiferromagnetic phase, using two different approaches. The first is perturbative in nature and relies on the fact that the nearest neighbor interaction energy between the dimers exceed the dimer hopping energy by a large factor of 8. We show that the system can approximately be treated as a non-interacting gas of kinks that behave like hard-core bosons. The second approach aims to describe long-range correlations employing the Luttinger-liquid theory. The relevant Luttinger parameter can be obtained by Bethe Ansatz solution of the equivalent XXZ spin model.

1. *Non-interacting kink approximation*

In Fig. 2 we plot the density distribution of dimers in a homogeneous lattice of $N_s = 99$ sites obtained from DMRG simulations with different number of dimers N. An infinite (hard-wall) confining potential $\epsilon_0 = \epsilon_{100} \to +\infty$ has been used, which imposes on Hamiltonian (1) open boundary conditions with $m_0 = m_{100} = 0$. Due to the asymmetric coupling at the boundaries, the end sites $j = 1$ and $j = 99$ prefer to be occupied with a particle. To accommodate an oscillating density wave, we therefore use odd number of lattice sites N_s. Note that the open boundary condition for the particles in Eq. (1) corresponds to an additional effective edge field $h_1 = h_{99} = -2$ for the spins in the XXZ-model of Eq. (3), which has the analogous effect of polarizing both end spins up.

As seen in Fig. 2, the ground state for $N = 50$ exhibits density oscillations corresponding to the AF Néel order, up to the small correction discussed in Sec. III B. Adding particles leads to modulated density distribution, with the envelope of modulation having regularly spaced nodes whose number is equal to twice the number of additional particles. In the following we will provide a simple theoretical understanding for this effect.

Without the small hopping term $\hat{H}_{\rm hop}$, the ground state of Hamiltonian (1) for half filling is the AF state $|\psi^{(0)}_{\rm AF}\rangle$ of Eq. (8), which is twofold degenerate. The AF order with period 2 effectively doubles the size of the unit cell. Adding then a particle to $|\psi^{(0)}_{\rm AF}\rangle$ costs exactly an energy of $(h+8)\tilde{J}$, resulting in state

$$|\ldots,\uparrow,\downarrow,\uparrow_j,\uparrow_{j+1},\uparrow,\downarrow,\uparrow,\downarrow,\uparrow,\ldots\rangle,$$

which is energy-degenerate with any state of the form

$$|\psi^{(0)}_{\rm AF+1}\rangle = |\ldots,\uparrow,\downarrow,\uparrow_j,\uparrow,\downarrow,\ldots,\downarrow,\uparrow_{j'},\uparrow,\downarrow,\ldots\rangle. \qquad (12)$$

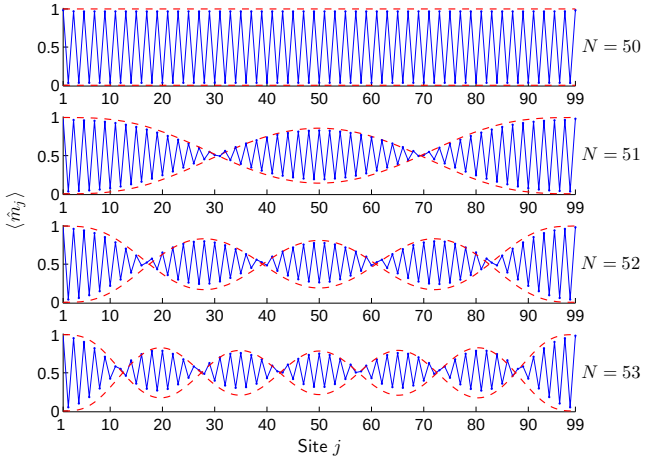

FIG. 2: (Color online) Particle density profile in a homogeneous lattice with $N_s = 99$ sites and hard-wall boundaries, for different particle number N. For half filling, $N = 50$, the ground state has nearly perfect AF order. Adding one, two and three particles leads to the density-wave modulations with the number of nodes equal twice the number of additional particles.

Hence, the additional particle causes effective domain walls, which can be placed anywhere in the system and play the role of mobile kinks at positions j and j' between AF regions with different orientation. Note that without hopping any number of particles above half filling can be created at the critical field $h_c^{(-)} = -8$ and placed in an arbitrary arrangement as long as no two neighboring lattice sites are empty. In other words, at $h_c^{(-)}$ we have a huge degeneracy of states with any magnetization $M_z \geq 0$ corresponding to arbitrary arrangement of antiferromagnetic regions and spin-up ferromagnetic regions. The analogous statement is also true at the upper critical field $h_c^{(+)} = 8$, where the degenerate subspace is defined as states with $M_z \leq 0$ where no two neighboring spins may point up. This degeneracy implies that without hopping the transition from the antiferromagnetic incompressible phase to the ferromagnetic incompressible phases is infinitely sharp at the effective critical magnetic fields $h_c^{(\pm)}$. As we will see below, however, the hopping lifts this degeneracy and therefore is crucial for the stability of compressible phases over finite ranges of field h as observed in Fig. 1.

The hopping $\hat{H}_{\rm hop}$ is also responsible for the modulated wave patterns seen in Fig. 2. Starting from the AF state in Eq. (8), we now insert more and more particles each producing a pair of kinks. The states in Eq. (12) can be considered as AF states with a pair of kinks, one at even sites and one at odd sites; e.g., state $|\downarrow_1,\uparrow_2,\downarrow_3,\uparrow_4,\uparrow_5,\uparrow_6,\downarrow_7,\uparrow_8,\downarrow_9,\ldots\rangle$ has kinks at sites 4 and 5, while state $|\downarrow_1,\uparrow_2,\downarrow_3,\uparrow_4,\uparrow_5,\downarrow_6,\uparrow_7,\uparrow_8,\downarrow_9,\ldots\rangle$ has kinks at sites 4 and 7. $\hat{H}_{\rm hop}$ has non-vanishing matrix elements within the subspace of energy degenerate

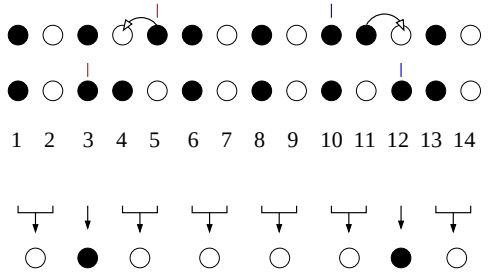

FIG. 3: (Color online) Top: 1D chain with one particle added to the AF state creating a pair of odd (red) and even (blue) kinks. The hopping Hamiltonian $\hat{H}_{\rm hop}$ leads to a motion of the odd and even kinks on odd or even sites, respectively. Interchange of odd- and even-site kinks is not possible. Bottom: mapping onto an effective lattice with lattice constant 2.

states with fixed number of additional particles. Within this manifold of states, hopping of the additional particle corresponds to free motion of kinks, wherein an even-site kink moves only on even sites and an odd-site kink on odd sites, as illustrated in the top part of Fig. 3. Furthermore, the even and odd site chain kinks cannot exchange their relative order. Note that hoping of a particle surrounded by two empty sites is energetically suppressed.

Given a fixed number of additional particles or holes, the motion of the corresponding kinks is equivalent to the motion of hard-core bosons in an effective lattice with lattice constant 2. To see this, consider the case of q additional particles on top of the half filled lattice; the opposite case of holes follows from the particle–hole symmetry. Let the positions of the kinks be $j_1 < j_2 < \ldots < j_{2q}$. If j_1 is even (odd) then $j_3, j_5, j_7, \ldots$ are also even (odd) and $j_2, j_4, j_6, \ldots$ are odd (even). We now perform a mapping onto a new lattice which we call the kink lattice. The quasi-position k_n of the nth kink is then

$$k_n = \begin{cases} \frac{j_n+n-1}{2} & \text{if } j_1 \text{ is even} \\ \frac{j_n+n}{2} & \text{if } j_1 \text{ is odd} \end{cases}. \tag{13}$$

This mapping is illustrated in the lower part of Fig. 3.

Evaluating the matrix elements of the hopping Hamiltonian $\hat{H}_{\rm hop}$ in the subspace of states with constant number of kinks, we find that the latter can be treated as hard-core bosons or non-interacting fermions on the kink lattice, only if we consider the absolute value of the wavefunction. The corresponding hopping strength on the period-2 lattice is again $\tilde{J}$. The exchange symmetry cannot be determined straightforwardly and therefore we employ this approximation only to determine the density distribution of dimers. For simplicity we choose the fermionic exchange symmetry.

Let us assume that the lattice is large and consider a particle filling close to the antiferromagnetic case. In this limit, the kinks can be regarded as moving on a continuum. This means that the dynamics of the kinks can now be determined by solving the Schrödinger equation for non-interacting fermions. For $N = \frac{1}{2}N_s + 1$, i.e., one additional particle, we have a pair of kinks whose ground-state wavefunction is

$$\Psi_2(x_1, x_2) = \frac{\sqrt{2}}{L}\left[\sin\frac{\pi x_1}{L}\,\sin\frac{2\pi x_2}{L} - \sin\frac{\pi x_2}{L}\,\sin\frac{2\pi x_1}{L}\right], \tag{14}$$

where $L = \frac{1}{2}N_s + 1$ is the length of the kink lattice. The left-most kink shall move on the odd sites. A particle is sitting on an even site j if and only if one chain kink is to the left of j. Thus the density of particles on the even sites is

$$\langle \hat{m}(x)\rangle = 2\int_0^x dy_1 \int_x^L dy_2\, \Psi_2^*(y_1, y_2)\Psi_2(y_1, y_2). \tag{15}$$

The prefactor of two emerges here because the integral occurs twice with interchanging the roles of y_1 and y_2. Although straightforward, we do not give the analytic expression of Eq. (15) since it is rather long. At the odd sites we get accordingly

$$\begin{aligned} 1 - \langle \hat{m}(x)\rangle \;=\; & \int_0^x dy_1 \int_0^x dy_2\, \Psi_2^*(y_1, y_2)\Psi_2(y_1, y_2) \\ & + \int_x^L dy_1 \int_x^L dy_2\, \Psi_2^*(y_1, y_2)\Psi_2(y_1, y_2). \end{aligned} \tag{16}$$

With q additional particles, the fermionic ground state wavefunction for $2q$ kinks is

$$\Psi_{2q}(x_1, \ldots, x_{2q}) = \sum_P \frac{\mathrm{sgn}(P)}{\sqrt{(2q)!}} \prod_{n=1}^{2q} \phi_{P(n)}(x_n), \tag{17}$$

where the sum is over all permutations P of numbers $\{1, 2, 3, \ldots, 2q\}$ and

$$\phi_n(x) = \sqrt{\frac{2}{L}}\,\sin\frac{\pi n x}{L},$$

with $L = \frac{1}{2}N_s + q$. This results in the density distribution

$$\begin{aligned} \langle \hat{m}(x)\rangle = & \sum_{k=0}^{q-1}\sum_{P,Q}\left[\frac{\mathrm{sgn}(P)\;\mathrm{sgn}(Q)}{(2k+1)!(2q-2k-1)!}\right. \\ & \left.\times \prod_{n=1}^{2k+1} I\big(0, x, P(n), Q(n)\big) \prod_{n=2k+2}^{2q} I\big(x, L, P(n), Q(n)\big)\right], \end{aligned} \tag{18}$$

where Q denotes the permutations of $\{1, 2, 3, \ldots, 2q\}$, and

$$I(a, b, n, m) = \int_a^b dx\, \phi_n^*(x)\phi_m(x),$$

with $n, m \in \{1, 2, 3, \ldots, 2q\}$. In Eq. (18) we have taken into account that there are $\frac{(2q)!}{(2q-2k-1)!(2k+1)!}$ possibilities of choosing $2k+1$ kinks to the left of j.

The dashed red lines in Fig. 2 show the analytic results for the particle density in a box potential with the lattice

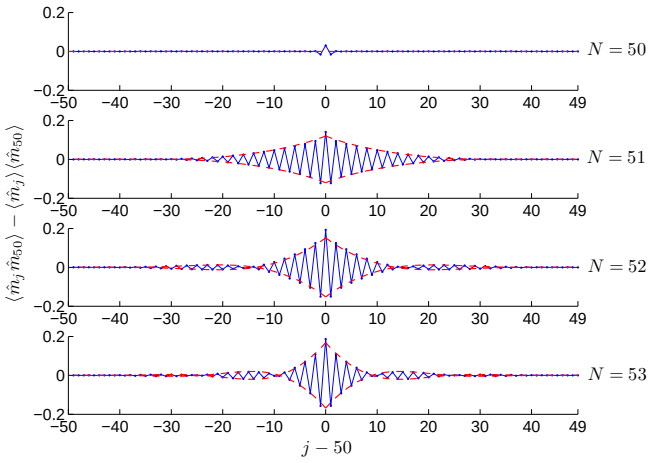

FIG. 4: (Color online) Particle density-density correlations in a homogeneous lattice with $N_s = 99$ sites and hard-wall boundaries, for different particle number N. The blue lines correspond to numerical DMRG results, the red dashed lines to the predictions of the kink approximation.

filling slightly above one half obtained from the kink approximation. The agreement with the numerical DMRG data is rather good. The kink model also explains in a very intuitive way the pairwise appearance of nodes with adding every particle to the lattice.

Particle number correlations can be derived in the same manner. For two even sites at positions j_1 and j_2, the configurations contributing to the correlations correspond to an odd number of particles to the left of j_1, an even number of particles between j_1 and j_2, and an even number of particles to the right of j_2. The particle density-density correlations are then given by

$$\langle \hat{m}(x)\hat{m}(y)\rangle = \sum_{\substack{k_1,k_2,k_3=0 \\ \leq (q-1)}}^{k_1+k_2+k_3} \sum_{P,Q} \Bigg[\frac{\mathrm{sgn}(P)\ \mathrm{sgn}(Q)}{(2k_1+1)!(2k_2)!(2k_3+1)!} \times \prod_{n=1}^{2k_1+1} I\big(0,x,P(n),Q(n)\big) \prod_{n=2k_1+2}^{2k_1+2k_2+1} I\big(x,y,P(n),Q(n)\big) \times \prod_{n=2k_1+2k_2+2}^{2q} I\big(y,L,P(n),Q(n)\big) \Bigg], \quad \text{for} \quad x < y. \tag{19}$$

In Fig. 4 we plot the density-density correlations obtained from DMRG calculations (blue solid line) and the kink model (dashed red lines), displaying very good agreement. We finally note that within the approximation of non interacting kinks, first order correlations exist only between neighboring sites. This perturbative model therefore can not accurately describe such correlations.

2. *Field theoretical approach*

The spin chain equivalent to the dimer Hamiltonian (1) in 1D is given by Eq. (4) with $\Delta = 4$ and open boundary conditions. At zero magnetization $M_z = 0$, the XXZ model (4) is gapped, since $\Delta > 1$. However, as described in Sec. III A, the gap can be closed by a field between the two critical values, $h_c^{(-)} < h < h_c^{(+)}$. In other words, the system is critical for any nonzero magnetization away from the fully magnetized case. In this regime, the leading low-energy effective theory is a Luttinger liquid with two parameters, the spin velocity v and Luttinger parameter K. These are functions of the magnetization per site $s^z = M_z/N_s$ and anisotropy Δ [12] (which for the particular dimer model here is fixed, $\Delta = 4$).

In order to calculate correlation functions, we first derive the Luttinger parameter $K(s^z)$ from the exact solution [13]. We write

$$K = \xi^2(b), \tag{20}$$

where the function $\xi(x)$ is determined by the integral equation

$$\xi(x) = 1 + \int_{-b}^{b} \kappa(x-y)\xi(y)\,dy, \tag{21}$$

with the kernel

$$\kappa(x) = \frac{1}{\pi}\frac{\sinh 2\eta}{\cos 2x - \cosh 2\eta}, \qquad \Delta = \cosh\eta > 1.$$

The parameter b in Eqs. (20) and (21) is implicitly defined through

$$s^z = \frac{1}{2} - \int_{-b}^{b} \rho(x)\,dx, \tag{22a}$$

$$\rho(x) = d(x) + \int_{-b}^{b} \kappa(x-y)\rho(y)\,dy, \tag{22b}$$

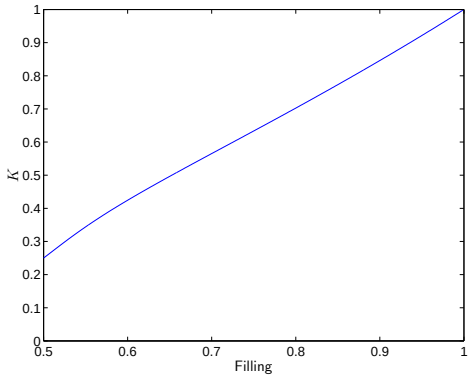

FIG. 5: Dependence of the Luttinger parameter K on the mean lattice filling N/N_s, for $\Delta = 4$.

where

$$d(x) = \frac{1}{\pi}\frac{\sinh\eta}{\cos 2x - \cosh\eta}, \qquad \Delta = \cosh\eta > 1.$$

Equations (20)-(22) are solved numerically by discretizing the integral and inverting the resulting matrix equation. Figure 5 shows the function $K(s^z)$ for $\Delta = 4$.

Within the Luttinger liquid approach, one- and two-point correlation functions can be calculated using the standard mode expansion of bosonic fields [14] for open boundary conditions [15, 17]. Then the spin-spin correlation function in the ground state reads

$$\begin{aligned}\langle \hat{S}^z(x)\hat{S}^z(y)\rangle \;=\; & (s^z)^2 - B\,\frac{K}{8(N_s+1)^2}\left(\frac{1}{\sin^2\frac{\pi(x-y)}{2(N_s+1)}}+\frac{1}{\sin^2\frac{\pi(x+y)}{2(N_s+1)}}\right) + C_1\,\frac{\cos\left[(2k_F+\theta/N_s)x+\varphi_1\right]}{\left(\sin\frac{\pi x}{N_s+1}\right)^K} \\ & + C_2\,\frac{\cos\left[(2k_F+\theta/N_s)y+\varphi_2\right]}{\left(\sin\frac{\pi y}{N_s+1}\right)^K} + D\,\frac{\cos\left[(2k_F+\theta/N_s)x+\delta\right]}{\left(\sin\frac{\pi x}{N_s+1}\,\sin\frac{\pi y}{N_s+1}\right)^K}\left[\frac{\sin\frac{\pi(x+y)}{2(N_s+1)}}{\sin\frac{\pi(x-y)}{2(N_s+1)}}\right]^{2K}, \end{aligned} \tag{23}$$

with the Fermi wavevector $k_F \equiv \pi(1-2s^z)/2$. Here the amplitudes $B, C_{1,2}, D$, the shift θ, and the phases $\varphi_{1,2}, \delta$ result from bosonization of operators on the lattice. We consider them as parameters in Eq. (23) that are fixed numerically by fitting to the DMRG data. The exponents, however, are obtained from the Luttinger liquid parameter K, which is given by the Bethe Ansatz. Figure 6 shows the remarkable agreement between the two approaches. Note the shift in the wavevectors of the oscillations by a constant θ that depends on the boundary conditions, the interaction and the magnetization. It has also been observed in the context of density oscillations in the open Hubbard model [16, 18].

The corresponding result for the first-order correlation function in the ground state is

$$\begin{aligned}\langle \hat{S}^+(x)\hat{S}^-(y)\rangle \;=\; & \left[\frac{\sqrt{\sin\frac{\pi x}{N_s+1}\,\sin\frac{\pi y}{N_s+1}}}{\sin\frac{\pi(x+y)}{2(N_s+1)}\,\sin\frac{\pi(x-y)}{2(N_s+1)}}\right]^{1/(2K)}\left(B\,\frac{\cos\left[(2k_F+\theta/N_s)(x-y)+\delta\right]}{\left(\sin\frac{\pi x}{N_s+1}\,\sin\frac{\pi y}{N_s+1}\right)^K}\left[\frac{\sin\frac{\pi(x+y)}{2(N_s+1)}}{\sin\frac{\pi(x-y)}{2(N_s+1)}}\right]^{2K}\right. \\ & \left. + C_1\,\frac{\cos\left[(2k_F+\theta/N_s)x+\varphi_1\right]}{\left(\sin\frac{\pi x}{N_s+1}\right)^K} + C_2\,\frac{\cos\left[(2k_F+\theta/N_s)y+\varphi_2\right]}{\left(\sin\frac{\pi y}{N_s+1}\right)^K}\right). \end{aligned} \tag{24}$$

Similarly to Eq. (23), the quantities $B, C_{1,2}, D, \delta, \phi_{1,2}, \theta$ are considered as fitting parameters. The resulting curves are shown in Fig. 7.

IV. PHASE DIAGRAM IN HIGHER DIMENSIONS

We now derive the phase boundaries for the dimer system in two and three dimensions. To that end, we employ the strong-coupling approach [19], wherein the hopping term $\hat{H}_{\rm hop} = -\tilde{J}\sum_{\langle j,i\rangle}\hat{c}_j^\dagger\hat{c}_i$ of Hamiltonian (1) is treated as small perturbation with respect to $\hat{H}_{\rm eff}^{(0)} \equiv \hat{H}_{\rm eff} - \hat{H}_{\rm hop}$.

a. Zero-hopping limit. Without the hopping, the grand canonical operator for the dimer system reads

$$\hat{H}_{\rm eff}^{(0)} = 4\tilde{J}\sum_{\langle j,i\rangle}\hat{m}_j\hat{m}_i - \mu\sum_j \hat{m}_j. \tag{25}$$

In this (formal) limit, the model is isomorphic to the Ising model in an external magnetic field and it has two critical points

$$\mu_\downarrow^{(0)}/\tilde{J} \;=\; 0, \tag{26a}$$

$$\mu_\uparrow^{(0)}/\tilde{J} \;=\; 16d. \tag{26b}$$

For very small values of the chemical potential, $\mu < 0$, all spins are polarized in the $-z$ direction, which in the dimer language corresponds to a state with zero dimers at each lattice site. For sufficiently large values of chemical potential, $\mu > 16d\tilde{J}$, all spins are aligned in the $+z$ direction, i.e., we have unit filling of the dimer lattice. Finally, for intermediate values of the chemical potential, $\mu_\downarrow^{(0)} < \mu < \mu_\uparrow^{(0)}$, the ground state is twofold degenerate and has antiferromagnetic order corresponding to a "checkerboard-crystal" lattice of dimers.

b. Boundaries of ferromagnetic phases. When the hopping term $\hat{H}_{\rm hop}$ is brought into the picture, the two critical points extend to two critical regions in which the system is compressible. In order to determine the chemical potentials at which the transitions between the compressible and incompressible ferromagnetic phases take

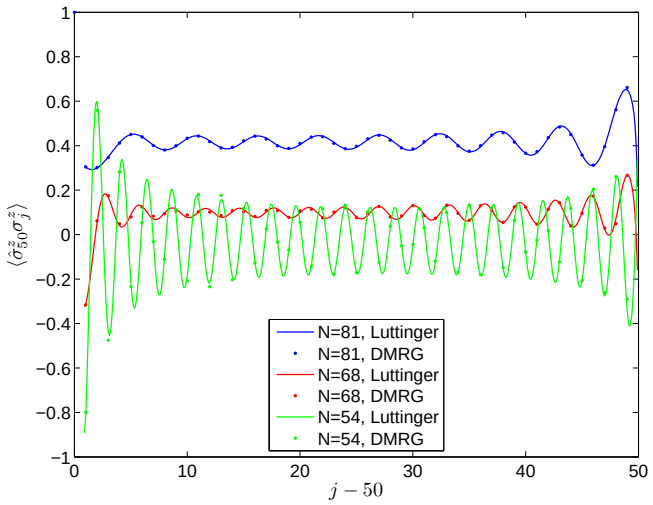

FIG. 6: (Color online) $\langle \hat{S}^z(x)\hat{S}^z(50)\rangle$ correlations obtained from the DMRG (dots) and the Luttinger-liquid approximation (solid lines).

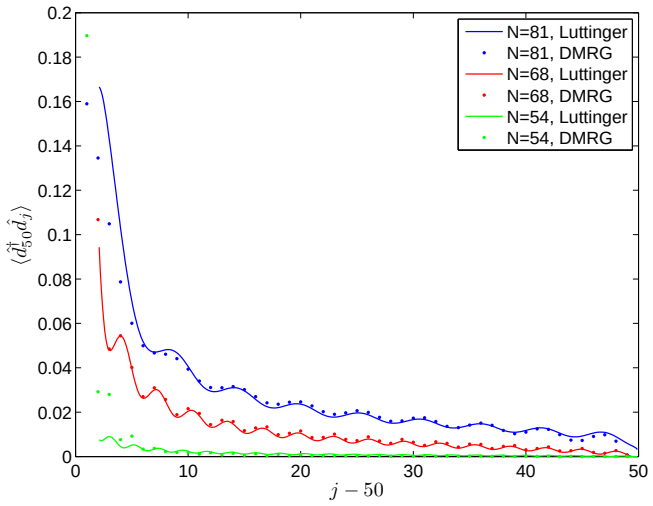

FIG. 7: (Color online) $\langle \hat{S}^+(x)\hat{S}^-(50)\rangle$ correlations obtained from the DMRG (dots) and the Luttinger-liquid approximation (solid lines).

place, we calculate the particle and hole excitation energies for zero and full filling of a finite lattice with even number of sites N_s using Hamiltonian (1).

In the case of a single dimer in an empty lattice, there is no contribution from the interaction energy and we find immediately without resorting to perturbative treatment

$$\begin{aligned} E(N=0) &= 0, \\ E(N=1) &= (U-2d\tilde{J})-2d\tilde{J}. \end{aligned}$$

In the filled lattice, each nearest neighbour link contributes $8\tilde{J}$ of repulsive interaction energy and we obtain

$$\begin{aligned} E(N=N_s) &= (U-2d\tilde{J})N_s+8d\tilde{J}N_s, \\ E(N=N_s-1) &= (U-2d\tilde{J})(N_s-1) \\ &\quad +8d\tilde{J}(N_s-2)-2d\tilde{J}. \end{aligned}$$

The critical chemical potentials, are then determined by the energy difference $E(1)-E(0)$, at which we add a dimer to the empty lattice, and $E(N_s)-E(N_s-1)$, at which we add a hole to (or remove a dimer from) the filled lattice

$$\mu_\downarrow/\tilde{J} = -2d, \tag{27a}$$
$$\mu_\uparrow/\tilde{J} = 18d. \tag{27b}$$

It should be noted that the hopping Hamiltonian does not modify the corresponding states in the two insulating phases, i.e., within the empty and fully-filled lattice phases there are no fluctuations of the dimer number, which is exactly zero or one per site, respectively.

c. Boundaries of antiferromagnetic phase. We now calculate the lower and upper critical chemical potentials $\mu_{\mathrm{AF}\mp}$ for the AF phase, up to the second order in dimer hopping. At exactly half filling, $N=\frac{1}{2}N_s$, the ground state is an almost perfect antiferromagnet with an alternating density structure in which there are no nearest-neighbour repulsive junctions between the dimers. However, due to $\hat{H}_{\mathrm{hop}}$ each dimer undergoes highly nonresonant transitions to the neighboring empty sites, whose number is $2d$ (see Fig. 8 illustrating the 2D case), and we obtain

$$E^{(2)}\left(\tfrac{1}{2}N_s\right)=(U-2d\tilde{J})\tfrac{1}{2}N_s-\frac{(\tilde{J})^2}{8\tilde{J}(2d-1)}\,\tfrac{1}{2}N_s\,2d,$$

where the last term describes the second-order energy shifts resulting from the virtual transitions of the dimers.

In the cases of $N=\frac{1}{2}N_s\pm 1$, the added dimer or dimer hole can not freely move for $d\geq 2$, since it would require two hopping events, as can be seen in Fig. 8. This should be contrasted with the 1D situation, wherein adding a dimer or a hole to the AF phase creates two mobile kinks,

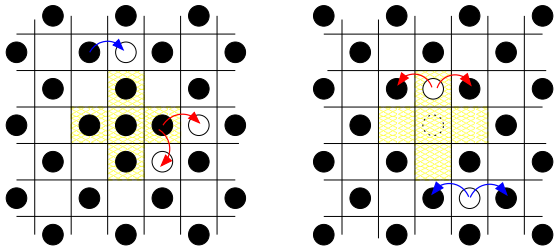

FIG. 8: (Color online) AF state in 2D lattice with an additional particle (left) or hole (right). Virtual hopping of particles (holes) adjacent to the defect (red) and in the bulk (blue) lead to different second-order energy contributions. Hopping of the additional particle or hole is not allowed.

discussed in Sec. III C 1. Taking into account the second order corrections due to virtual transitions of dimers adjacent to the extra dimer or dimer-hole (see Fig. 8 left or right, respectively), we obtain

$$\begin{aligned} E^{(2)}\left(\tfrac{1}{2}N_s \pm 1\right) &= (U - 2d\tilde{J})\left(\tfrac{1}{2}N_s \pm 1\right) \\ &\quad - \frac{(\tilde{J})^2}{8\tilde{J}(2d-1)}\left(\tfrac{1}{2}N_s - 2d\right)2d \\ &\quad - \frac{(\tilde{J})^2}{8\tilde{J}(2d-2)}\,2d\,(2d-1). \end{aligned}$$

The lower $\mu_{\mathrm{AF}-} = E^{(2)}\left(\frac{1}{2}N_s\right) - E^{(2)}\left(\frac{1}{2}N_s - 1\right)$ and upper $\mu_{\mathrm{AF}+} = E^{(2)}\left(\frac{1}{2}N_s + 1\right) - E^{(2)}\left(\frac{1}{2}N_s\right)$ critical chemical potentials for the AF phase in $d \geq 2$ dimensions are then given by

$$\mu_{\mathrm{AF}-}/\tilde{J} = \frac{d}{4(2d-1)(2d-2)}, \tag{28a}$$

$$\mu_{\mathrm{AF}+}/\tilde{J} = 16d - \frac{d}{4(2d-1)(2d-2)}. \tag{28b}$$

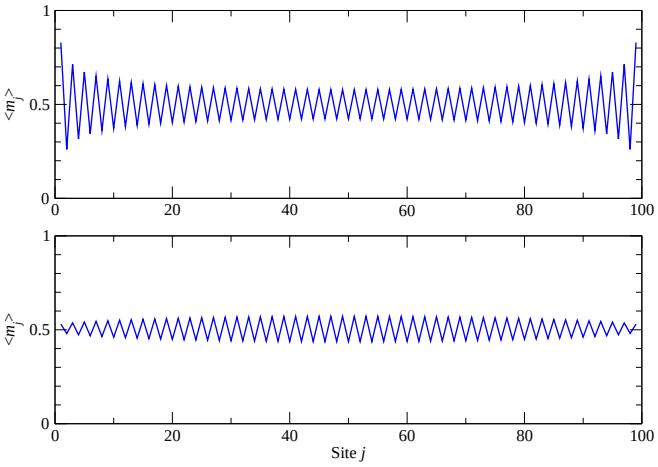

FIG. 9: Top: Ground state density profile in a homogeneous lattice with $N_s = 99$ sites and hard-wall boundaries, for $N = 50$ particles, but with hopping strength equal to the nearest neighbor repulsion, $\Delta = 1$ (compare to Fig. 2, top panel). Bottom: The same, but without the effective edge fields in the spin chain model.

V. THE ROLE OF ANISOTROPY Δ

The effective Hamiltonian (1) has a fixed relation of the nearest neighbour interaction to hopping, which results in a fixed Ising like anisotropy $\Delta = 4$ in Eq. (3). It is now interesting to also consider the more general case of tunable anisotropy, which could for example be realized with dimers consisting of two different atomic species [20]. As the hopping becomes stronger, the perturbative analysis used in the previous sections becomes unreliable. It is known that the model of Eq. (4) is critical for $-1 \leq \Delta \leq 1$. Therefore, the perturbation treatment breaks down exactly at the point where the hopping becomes equal to or larger than the nearest neighbor dimer-dimer interaction. However, it is still possible to use the field theoretical methods of Sec. III C 2 to calculate the correlation functions and expectation values.

In the critical region excitations are gapless in the thermodynamic limit, so that there is no incompressible phase at half-filling. The crossover between the completely filled and completely empty regions in Fig. 1 is therefore continuous as a function of the effective field and there is no extended half-filled phase. The strength of hopping is therefore crucial for the behavior of the system: weak hopping enables the presence of a compressible phase between the incompressible ferromagnetic and antiferromagnetic phases. With increasing the hopping strength the incompressible antiferromagnetic phase shrinks and completely vanishes when the hopping reaches the value of the nearest neighbor interaction, $\Delta \leq 1$.

Equally interesting is the effect of hopping on the density of dimers along the chain. As discussed in Sec. III C, density-wave modulations appear in Fig. 2 because of the effective motion of kinks. The complex interplay between the kinetic and interaction terms in the critical region now leads to a further modification of the density pattern along the chain [21–23]. In particular, the amplitude of the ground state density oscillations is now significantly reduced towards the middle of the chain with a characteristic drop-off as shown in Fig. 9. Excited states with larger N would then exhibit modulations on top of this ground state pattern, similar to Fig. 2.

Interestingly, the exact form of the boundary conditions play now a much more important role. Namely, the effective edge field of the spin chain model discussed in Sec III C 1 accounts for a large part of the ground state density oscillations. For comparison, in Fig. 9 we also show the density for the spin chain model without any edge field. The density amplitude is now smaller near the boundary. At $\Delta = 1$, this amplitude has been predicted to follow approximately a $\sqrt{\sin(\pi x/N_s)}$ behavior [21], which however is strongly affected by temperature [22, 23] due to the gapless modes.

VI. SUMMARY

In this paper, we have studied the many-body dynamics of attractively bound pairs of atoms in the Bose-Hubbard model. When the on-site interaction between the atoms exceeds by a sufficient amount the bandwidth of the lowest single-particle Bloch band, the pairs are well co-localized and can be treated as composite dimer particles. Then the effective model for dimers on a lattice is equivalent to an asymmetric spin-$\frac{1}{2}$ XXZ model in an external magnetic field: the nearest neighbor interaction between the dimers translates into an Ising-type spin-spin interaction and the dimer tunneling to a spin-spin coupling in the $x - y$ plane.

The case of repulsively bound pairs studied in [9] corresponds to a ferromagnetic Ising coupling. In contrast, for attractively bound pairs analyzed here, the Ising coupling is antiferromagnetic leading to a much richer phase diagram. The asymmetry parameter Δ of the XXZ model is equal to 4; as a result, the system is gapped for both zero and full magnetization. The zero magnetization state, corresponding to exactly half filling of dimers, exhibits antiferromagnetic order, while the full magnetization (ferromagnetic) states correspond to vanishing or full filling of dimers. When the effective magnetic field, or for that matter the chemical potential for the dimers, exceeds critical values, the gap is closed and the dimer system becomes critical with finite compressibility.

We have derived the critical values of the chemical potential for the transition points from the gapped ferromagnetic and antiferromagnetic phases to the compressible phases in 1D, employing the known exact solutions of the XXZ model, and by using a strong-coupling approximation in higher dimensions. The properties of the compressible phases are quite different in one and higher spatial dimensions. In 1D, close to half filling, the system can be well described by kink-like domain walls which separate antiferromagnetic strings of opposite phase and can propagate through the lattice almost freely. In higher dimensions, the motion of similar defects is strongly suppressed. A simple approximate description in terms of non-interacting kinks gives rather accurate predictions for the dimer density as well as non-local density-density correlations.

In order to explain the first order correlations, we employed a field theoretical approach based on the Luttinger liquid theory. The corresponding Luttinger parameter was obtained by solving the Bethe Ansatz equations for the equivalent XXZ model in the regime of critical magnetic fields. The expressions for the first-order and density-density correlations showed remarkably good agreement with the numerical data obtained by DMRG simulations. Finally we discussed the consequences of changing the anisotropy parameter of the XXZ model. Our studies attest that interaction bound pairs of atoms in deep optical lattices can provide a versatile tool to simulate and explore quantum spin models.

Acknowledgments

We are thankful for discussions with Fabian Essler, Manuel Valiente and Xue-Feng Zhang. This work was supported by the EU network EMALI and the DFG through the SFB TR49.

[1] A.L. Fetter and J.D. Walecka, *Quantum Theory of Many Particle Systems* (McGraw-Hill, New York, 1971); N.J. Ashcroft and and N.D. Mermin, *Solid State Physics* (International Thomson Publishing, New York, 1976).
[2] R. Micnas, J. Ranninger, and S. Robaszkiewicz, Rev. Mod. Phys. **62**, 113 (1990).
[3] O. Morsch and M. Oberthaler, Rev. Mod. Phys. **78**, 179 (2006); I. Bloch, J. Dalibard, and W. Zwerger, Rev. Mod. Phys. **80**, 885 (2008); M. Lewenstein, A. Sanpera, V. Ahufinger, B. Damski, A. Sen De, and U. Sen, Adv. Phys. **56**, 243 (2007).
[4] D. Jaksch, C. Bruder, J.I. Cirac, C.W. Gardiner, and P. Zoller, Phys. Rev. Lett. **81**, 3108 (1998); M. Greiner, O. Mandel, T. Esslinger, T.W. Hänsch, and I. Bloch, Nature **415**, 39 (2002); D. Jaksch and P. Zoller, Ann. Phys. (N.Y.) **315**, 52 (2005).
[5] G. Thalhammer, K. Winkler, F. Lang, S. Schmid, R. Grimm, and J. Hecker Denschlag, Phys. Rev. Lett. **96**, 050402 (2006); T. Volz, N. Syassen, D.M. Bauer, E. Hansis, S. Dürr, and G. Rempe, Nature Phys. **2**, 692 (2006).
[6] K. Winkler, G. Thalhammer, F. Lang, R. Grimm, J. Hecker Denschlag, A.J. Daley, A. Kantian, H.P. Büchler, and P. Zoller, Nature **441**, 853 (2006); J. Hecker Denschlag and A.J. Daley, arXiv:cond-mat/0610393.
[7] R. Piil and K. Mølmer, Phys. Rev. A **76**, 023607 (2007); N. Nygaard, R. Piil, and K. Mølmer, Phys. Rev. A **78**, 023617 (2008).
[8] M. Valiente and D. Petrosyan, J. Phys. B **41**, 161002 (2008).
[9] D. Petrosyan, B. Schmidt, J.R. Anglin, M. Fleischhauer, Phys. Rev. A **76**, 033606 (2007); *ibid.* **77**, 039908(E) (2008).
[10] C.N. Yang and C.P. Yang, Phys. Rev. **150**, 327 (1966).
[11] S.R. White, Phys. Rev. Lett. **69**, 2863 (1992); U. Schollwoeck, Rev. Mod. Phys. **77**, 259 (2005).
[12] F.D.M. Haldane, Phys. Rev. Lett. **45**, 1358 (1980).
[13] A.G. Izergin and V.E. Korepin, Nucl. Phys. B **275**, 687 (1986).
[14] S. Eggert in *Lecture Note: Theoretical Survey of one dimensional wire systems*, Proceedings of 2006 A3 Summer school on physics and chemistry.
[15] S. Eggert and I. Affleck, Phys. Rev. B **46**, 10866 (1992).
[16] S. Söffing, M. Bortz, I. Schneider, A. Struck, M. Fleischhauer and S. Eggert, arXiv:0808.0008.
[17] M.A. Cazalilla, J. Phys. B **37**, S1 (2004).
[18] G. Bedürftig, B. Brendel, H. Frahm and R. M. Noack, Phys. Rev. B **58**, 10225 (1998)
[19] J.K. Freericks and H. Monien, Phys. Rev. B **53**, 2691 (1996).
[20] M. Valiente and D. Petrosyan (to be published).
[21] S. Eggert, I. Affleck, and M.P.D. Horton, Phys. Rev. Lett. **89**, 47202 (2002); Phys. Rev. Lett. **90**, 89702 (2003).
[22] S. Eggert and I. Affleck, Phys. Rev. Lett. **75**, 934 (1995).
[23] S. Rommer and S. Eggert, Phys. Rev. B **62**, 4370 (2000).